Net Mn moment due to canted spins at $SrRuO_3/SrMnO_3$ interfaces

Y. Choi,[1,a)] Y. Z. Yoo,[2] O. Chmaissem,[2] A. Ullah,[2] S. Kolesnik,[2] C. W. Kimball,[2] D. Haskel,[3] J. S. Jiang,[1] and S. D. Bader[1]
[1]*Materials Science Division, Argonne National Laboratory, Argonne, Illinois 60439, USA*
[2]*Institute for NanoScience, Enginering, and Technology, Physics Department, Northern Illinois University, DeKalb, Illinois 60115, USA*
[3]*Advanced Photon Source, Argonne National Laboratory, Argonne, Illinois 60439, USA*

(Presented on 8 November 2007; received 9 September 2007; accepted 16 October 2007; published online 14 February 2008)

A net moment was observed from Mn in a $SrRuO_3/SrMnO_3$ (SRO/SMO) superlattice film via element-specific x-ray resonant magnetic techniques. The collective magnetic behavior of the SRO and SMO layers is significantly modified by their exchange interaction. Bulk magnetometry shows a two-step, easy-axis magnetization reversal process, and x-ray measurements reveal that the reversal with higher coercivity involves the magnetization in the SMO layers. The results provide strong evidence for the presence of pinned SRO magnetization at the SRO/SMO interface. X-ray measurements and micromagnetic simulations reveal that the net Mn moment is due to a canted antiferromagnetic spin configuration in the SMO layers. © *2008 American Institute of Physics*. [DOI: 10.1063/1.2830962]

In nanoscale structures, combinations of materials with dissimilar properties are often forced to coexist. Recently, oxides with the perovskite structure have received much attention due to their tunable lattice parameters and flexibility in accommodating similarly-structured materials but with dissimilar properties. This type of system enables material designs for multifunctional devices and opens the possibility for materials with exotic properties. Taking advantage of coupling between orbital and spin degrees of freedom together with interfacial effect, strongly correlated transition metal oxides have potential applications as field effect transistors[1] and magnetic tunnel junctions.[2]

Perovskite $SrRuO_3$ (SRO) is an itinerant ferromagnet ($T_C \sim 163$ K),[3,4] whose magnetic and electronic properties can be readily tuned by substitution at Sr and/or Ru sites.[5] $SrMnO_3$ (SMO) is a G-type antiferromagnet with perovskite structure and a Néel temperature T_N of ~260 K.[6] High quality SRO/SMO superlattices can be grown on $SrTiO_3$ (STO) substrates due to a small lattice mismatch.[7] Grown on STO (100) substrates, the ferromagnetic SRO layers exhibit uniaxial anisotropy along the SRO[110] axis (the film normal direction),[8] while the antiferromagnetic SMO layers are expected to have their antiferromagnetically aligned spins in plane.

Because of the strong interaction between the SRO and SMO layers at the interfaces, the magnetization reversal of SRO/SMO superlattices can be significantly changed. For example, it was observed that each SRO layer divides into a free internal and two pinned near-interface layers during the magnetization reversal.[9,10] Similarly, the interfacial magnetic interactions may also modify the magnetic response of the SMO layers. However, the direct magnetic measurement of the antiferromagnetic SMO layers is not trivial because of the dominant magnetic contributions of the SRO layers. Here, we report a magnetization reversal study of the SMO layers using element-specific, x-ray resonant magnetic characterization techniques. The Mn-specific magnetic measurements, in combination with bulk-sensitive superconducting quantum interference device (SQUID) magnetometry measurements, reveal the response of the SMO layers during the magnetization reversal of the SRO layers.[11] Our results, coupled with micromagnetic simulations, allow us to provide a detailed picture on how the interactions at the interfaces modify the magnetic properties of both the SRO and SMO layers.

A single-crystalline $(SRO/SMO)_{19}$ superlattice film was grown on a STO (100) substrate by pulsed laser deposition.[12] Each SRO layer consisted of ten unit cells and each SMO layer consists of two unit cells. The superlattice was capped with an extra SRO layer to prevent possible SMO degradation. In order to study the magnetic response of the SMO layers, x-ray magnetic circular dichroism (XMCD) and x-ray resonant magnetic scattering (XRMS) measurements[13] were carried out at the Mn $L_{2,3}$ absorption edges. While the SQUID measurement provides the magnetic response of the whole sample, the XMCD and XRMS measurements provide Mn-specific magnetic information. X-ray measurements were performed at beamline 4-ID-C of the Advanced Photon Source at Argonne National Laboratory.[14]

The temperature dependence of the dc magnetization was measured using SQUID after zero field cooling with an applied field of 1 kOe parallel to the film surface normal (i.e., the magnetic easy axis of the SRO layers), as shown in Fig. 1. The Curie temperature of our superlattice is close to the bulk value of 163 K. With applied field along the easy axis of the SRO/SMO film, the field dependence was measured at 50 K via SQUID, as shown in Fig. 2(a). The SQUID hysteresis loop shows a two-step magnetization reversal process ($\Delta M1$ and $\Delta M2$).

[a)]Also at Department of Physics, University of Texas at Arlington, Arlington, Texas 76019. Electronic mail: yschoi@anl.gov.

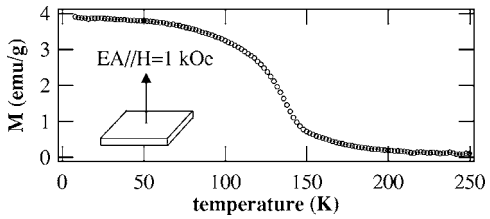

FIG. 1. Easy-axis (EA) SQUID result with an applied field H in the film normal direction.

The magnetic characterization of the SMO layers along the easy axis was carried out by measuring the field dependence of the Mn-XMCD signal, as shown in Fig. 2(b). Measurements were performed with the magnetic field applied parallel to the x-ray propagation direction, which is along the film normal. XMCD signals were measured in total electron yield (TEY) and helicity-switching mode. The result in Fig. 2(b) is unusual considering that XMCD signals are expected to be zero from typical antiferromagnets. Since XMCD is proportional to the ferromagnetic moment of resonant atoms projected along the x-ray propagation direction, the observed XMCD signal indicates that the Mn atoms have a net ferromagnetic moment in out-of-plane direction.

The Mn-specific XMCD data show a single step reversal with a coercive field of ~3.4 kOe that matches the coercive field of the high field reversal ΔM2 in the SQUID data. This suggests that the interfacial SRO regions, coupled to the spins in the SMO layers, are responsible for the enhanced coercivity of the superlattice relative to that of a single SRO layer (1.5 kOe at 5 K). The magnetization change ΔM2 is too big to be attributed to the SMO magnetization reversal only. The low field reversal ΔM1 is due to the switching of free SRO layers, whereas the high field reversal ΔM2 is due to the switching of pinned regions at the SRO/SMO interface. The higher field reversal process involves a simultaneous reversal of pinned SRO and SMO regions, as a result of the strong coupling at the SRO/SMO interface. In Fig. 2(b) an abrupt reversal of the SMO magnetization indicates a sudden change in the Mn spin configuration. The net magnetization in the SMO layer is a small fraction of the total magnetization in the SQUID data, since the total thickness of the SMO is about a factor of 5 smaller than that of the SRO. This is evidenced by saturation of magnetization above ~5 kOe [Fig. 2(a)] as compared to the steep field dependence of the net Mn magnetization [Fig. 2(b)]. To investigate this further, we carried out in-plane, field-dependent SQUID magnetometry and Mn-XRMS measurements, as shown in Figs. 2(c) and 2(d). The net Mn moment increases with the applied field [Fig. 2(d)]. In Fig. 2(d), the in-plane Mn-XRMS loop does not show hysteresis or remanent magnetization, in contrast to the out-of-plane loops of Fig. 2(b). This implies that the in-plane direction, nominally the easy direction for SMO grown on STO (100) substrates, is not the easy axis of the SMO in contact with the SRO layers.

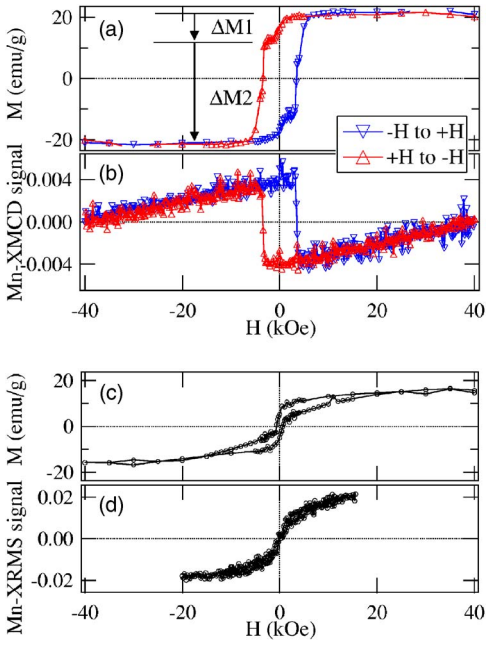

FIG. 2. (Color online) Out-of-plane magnetization measurements at 50 K via (a) SQUID and (b) Mn-specific XMCD. The XMCD signal is defined as $(I^+-I^-)/(I^++I^-)$, where $I^{+,-}$ are the TEYs for the two opposite polarizations of the incoming x rays. In-plane magnetization measurements via (c) SQUID and (d) Mn-specific XRMS. Instead of the TEYs, reflected intensities at 10° incident angle are used for the XRMS signal. The magnitude of XRMS and XMCD signals cannot be directly compared because the XRMS is affected by charge scattering.

The observed net moment in the SMO layers that results in nonzero signals in XMCD and XRMS measurements is either due to a ferromagnetic or canted antiferromagnetic arrangement of Mn spins. The out-of-plane Mn-XMCD hysteresis loop in Fig. 2(b) shows a linear suppression of the projected Mn moment as a function of increasing magnetic field. This unexpected behavior indicates that the SMO layers are not likely to be ferromagnetic. In the case of a canted antiferromagnet, the net projected moment would increase as a function of increasing field if the net moment and the field were aligned in the same direction. However, if the projected Mn moment is antiparallel to the SRO magnetization direction, then the opposite would occur. This latter scenario is consistent with our results and suggests that the exchange coupling between the Ru and Mn moments across the SRO/SMO interfaces is antiferromagnetic, as observed in Mn/Ru superlattices,[15] Mn-doped $SrRuO_3$,[5] and $SrRu_{0.9}Mn_{0.1}O_3$ polycrystals.[16] In agreement with the deduced antiferromagnetic coupling between Ru and Mn across the interfaces in our SRO/SMO system, antiferromagnetic exchange coupling between two magnetic layers was also found in $La_{0.67}Sr_{0.33}MnO_3/SrRuO_3$ bilayers[17] and in $La_{0.7}Sr_{0.3}MnO_3/SrRuO_3$ superlattices.[18]

Using micromagnetic calculations,[19] we studied possible spin configurations that give rise to the observed Mn moment in Fig. 2(b). The exchange constants J were estimated in the frame of the mean-field theory, $J=3k_BT_C/2zS(S+1)$, with $S(Mn^{4+})=1.5$ and $S(Ru^{4+})=1$ and bulk T_C(SRO) and T_N(SMO).[3–6] J values were calculated relative to J(Fe) so that $J(SRO)=J(Fe)/6.52$ and $J(SMO)=-2.925J(SRO)$. Magnetization of the SRO layers M_S(SRO) was measured to be 300 emu/cc, and M_S(SMO) was assumed to be 450 emu/cc, based on the ratio of $S(Mn^{4+})$ and $S(Ru^{4+})$. Anisotropy constant of the SRO layer K(SRO) was estimated to be 1.6×10^6 erg/cm.[4] It was assumed that K(SMO)

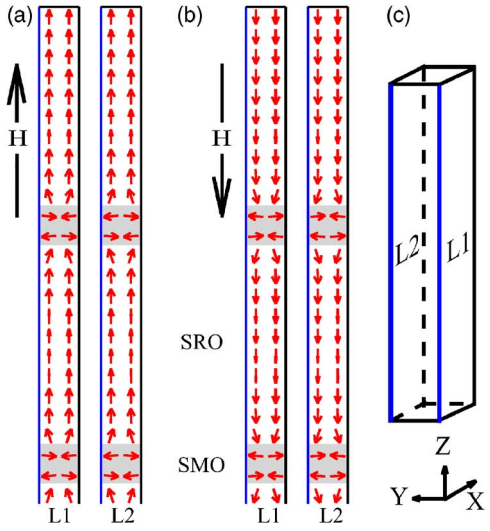

FIG. 3. (Color online) Simulated SRO/SMO spin configurations at ±30 kOe. The large arrows indicate the applied field direction. The shaded areas represent SMO layers. *L*1 and *L*2 indicate two cross-sectional views as illustrated in (c). Only top two bilayers out of the ten simulated bilayers are shown.

$=K(\mathrm{SRO})$ due to the lack of detailed information available for the antiferromagnet. Only the top half of the superlattice was simulated, since the top and bottom halves were symmetric. The total simulated volume was $0.8\times0.8\times47.6$ nm^3 with periodic conditions in the *x* and *y* directions [Fig. 3(c)]. The simulation cell size was $0.4\times0.4\times0.4$ nm^3. Parts of spin configurations at ±30 kOe are presented in Fig. 3, where two cross-sectional views in the *xz* plane are shown. Consistent with our analysis of the experimental result, the net Mn moment is antiparallel to the applied field direction and undergoes an abrupt reversal as the neighboring SRO layer reverses the magnetization direction. Although qualitative, this agreement is remarkable and yet fortuitous, considering that there was no adjustment to the material parameters.

The collective magnetic behavior of the dissimilar SRO and SMO layers is significantly modified due to their proximity. A comparative study of bulk- and Mn-sensitive magnetic measurements suggests the presence of pinned SRO layers near the interfaces and provides evidence of canting of the Mn spins in the SMO layers as a result of the competition between anisotropy and antiferromagnetic exchange coupling interactions at the SRO/SMO interface.

Work at NIU was supported by the Institute for Nano-Science, Engineering and Technology–U.S. Department of Education. Work at Argonne National Laboratory was supported by U.S. Department of Energy, Office of Science, under Contract No. DE-AC02-06CH11357.

[1] C. H. Ahn, S. Gariglio, P. Paruch, T. Tybell, L. Antognazza, and J.-M. Triscone, Science **284**, 1152 (1999).
[2] H. Yamada, Y. Ogawa, Y. Ishii, H. Sato, H. Akoh, M. Kawasaki, and Y. Tokura, Science **305**, 646 (2004).
[3] A. Callaghan, C. W. Moeller, and R. Ward, Inorg. Chem. **5**, 1572 (1966).
[4] A. Kanbayasi, J. Phys. Soc. Jpn. **41**, 1876 (1976).
[5] G. Cao, S. Chikara, X. N. Lin, E. Elhami, V. Durairaj, and P. Schlottmann, Phys. Rev. B **71**, 035104 (2005).
[6] T. Takeda and S. Ohara, J. Phys. Soc. Jpn. **37**, 275 (1974); O. Chmaissem, B. Dabrowski, S. Kolesnik, J. Mais, D. E. Brown, R. Kruk, P. Prior, B. Pyles, and J. D. Jorgensen, Phys. Rev. B **64**, 134412 (2001).
[7] P. Padhan, W. Prellier, and B. Mercey, Phys. Rev. B **70**, 184419 (2004).
[8] Y. Z. Yoo, O. Chmaissem, S. Kolesnik, A. Ullah, L. B. Lurio, D. E. Brown, J. Brady, B. Dabrowski, C. W. Kimball, M. Haji–Sheikh, and A. P. Genis, Appl. Phys. Lett. **89**, 124104 (2006).
[9] P. Padhan and W. Prellier, Phys. Rev. B **72**, 104416 (2005).
[10] P. Padhan and W. Prellier, Appl. Phys. Lett. **88**, 263114 (2006).
[11] Y. Choi, Y. Z. Yoo, O. Chmaissem, A. Ullah, S. Kolesnik, C. W. Kimball, D. Haskel, J. S. Jiang, and S. D. Bader, Appl. Phys. Lett. **91**, 022503 (2007).
[12] Y. Z. Yoo, O. Chmaissem, S. Kolesnik, B. Dabrowski, M. Maxwell, C. W. Kimball, L. McAnelly, M. Haji–Sheikh, and A. P. Genis, J. Appl. Phys. **97**, 103525 (2005).
[13] C. Kao, J. B. Hastings, E. D. Johnson, D. P. Siddons, G. C. Smith, and G. A. Prinz, Phys. Rev. Lett. **65**, 373 (1990).
[14] J. W. Freeland, J. C. Lang, G. Srajer, R. Winarski, D. Shu, and D. M. Mills, Rev. Sci. Instrum. **73**, 1408 (2001).
[15] V. Dupuis, M. Maurer, M. Piecuch, M. F. Ravet, J. Dekoster, S. Andrieu, J. F. Bobo, F. Baudelet, P. Bauer, and A. Fontaine, Phys. Rev. B **48**, 5585 (1993).
[16] Z. H. Han, J. I. Budnick, W. A. Hines, B. Dabrowski, and T. Maxwell, Appl. Phys. Lett. **89**, 102501 (2006).
[17] X. Ke, M. S. Rzchowski, L. J. Belenky, and C. B. Eom, Appl. Phys. Lett. **84**, 5458 (2004).
[18] P. Padhan, W. Prellier, and R. C. Budhani, Appl. Phys. Lett. **88**, 192509 (2006).
[19] Using the LLG micromagnetics simulator.